BENIN JOURNAL OF PHYSICAL SCIENCES
BJPS Vol. 1(1), June, pg. 42-51 (2024)
www.bjps.org.ng

Insight into the structure and work function of the (100) surface of diamond-like Carbon: A first-principles calculation

O. R. JOLAYEMI and S. D. TOBIN-WEST

Department of Physics, College of Science & Technology, Covenant University, Ogun State, Nigeria

Received: 08/05/2024 ***Accepted:*** 28/05/2024

Abstract

We study the work function of low index surface (100) of diamond (face-centered) carbon using pseudopotential plane-wave density functional calculations with the generalized gradient approximation. We consider clean, unrelaxed surfaces in the slab-supercell approximation at 0 K. Particular attention is paid to the convergence of the vacuum in the slab model with respect to slab thickness. The obtained work function, 7.53 eV, shows a slight deviation from the experimental value. Including temperature effect, surface relaxation, and possible surface reconstruction may improve computational results compared to experiments.

Keywords: *Diamond Carbon, Work function, DFT, Slab*

1. INTRODUCTION

Carbon exists in multiple allotropes, including graphite, diamond, and graphene, and exhibits diverse electronic properties. Diamond, one of Carbon's most ancient allotropic structures, possesses several remarkable characteristics that can be utilized in high-power electronic applications, even under extreme voltage, temperature, and frequency (Endo *et al*., 2003). With an operational temperature five times that of silicon and a Debye temperature of 2000 K (Rivero *et al*., 2016), it surpasses the Debye temperature of most other insulating materials by an order of magnitude. Due to its substantial electronic band gap, diamond possesses a breakdown field strength 20 times greater than mica, a material frequently employed in capacitors. This quality makes Carbon in the diamond structure suitable for high-voltage insulation in thin layers. Furthermore, it exhibits

*Corresponding author, e-mail: omamuyovwi.jolayemi@covenantuniversity.edu.ng

remarkable transport properties, including a charge carrier mobility of approximately 3000 cm^2/Vs and the highest thermal conductivity of any material at room temperature, surpassing that of copper by a factor of five (Rivero *et al.,* 2016) .

The work function refers to the minimum energy required to extract an electron from within a material's bulk, pass it through a surface, and relocate it outside the material (Singh-Miller and Marzari, 2009). Experimental measurement techniques for determining material work functions can be broadly categorized into two groups. The electron emission process is the basis of the first category. Here, an absolute scale is used to measure the work function. Different techniques are used to simulate a material's surface, which encompasses photoemission (like the photoelectric effect and ultraviolet photoelectron spectroscopy), field emission (using an applied electric field), thermal emission (thermionic emission) (Olawole *et al.,* 2021), or a blend of these methods. Another category involves evaluating variations in work function among diverse metals (e.g., Kelvin probe force microscopy) or when undergoing surface modifications comparable to adsorption procedures (Olawole *et al.,* 2022). When using these techniques, work function measurements are typically relative and often necessitate standard reference work function calculations.

Computational, the work function is obtainable in two ways (Singh-Miller and Marzari, 2009):

1) Calculating directly the difference between the potential in the vacuum region and the Fermi energy of the slab.
2) By referencing the macroscopic average of the potential of the slab's interior to that of a bulk calculation and taking the difference of the V_{vacuum} of the slab and E_{fermi} of the bulk.

In this study, we will explore through a computational approach the structural properties and work function of the (100) surface of carbon in a diamond lattice, which is a nonmetallic FCC material. The (100) plane is often one of the most symmetric and simple crystallographic planes, making it an ideal choice for initial investigations or fundamental studies. The symmetry is the same for the (010) and (001) planes. Surface science and material interactions often focus on the (100) plane due to its frequent exposure in real-world applications. We chose this plane to simplify the studies. Density Functional Theory (DFT) utilizing the generalized-gradient-approximation (GGA) method will be used for the investigation.

2. MATERIALS AND METHOD

The slab model involves constructing a supercell of layered slabs of solid material with gaps of empty space in between. These gaps, often called vacuum space,

create a separation between recurring replicas of the slab along the z-axis. The modeling involves asymmetrical slabs with (100) surfaces (Jolayemi *et al*., 2021), comprising slab thickness separated by a 8.8904 Å vacuum gap, equivalent to 5 interlayer distances. Our test calculations demonstrate that this inter-slab distance is sufficiently extensive to prevent unintended interactions among the replicated slabs in the z-direction. The supercell method was employed, utilizing unit cells with $1 \times 1 \times n$ $(n = 1, 2, 3, \ldots, 15)$.

The Quantum ESPRESSO (QE) (Giannozzi *et al*., 2009) codes were used for the calculations, relying on the Plane-Wave Density Functional Theory. To represent the valence electrons ($2s^2\ 2p^2$electrons), a scalar-relativistic pseudopotential combined with plane wave method were used. The PBE exchange-correlation (GGA) functional (Perdew *et al*., 1996, 1997) was chosen for the calculations. The wave-function cut-off was fixed at 45 Ry following the convergence test from Figure 1, with a corresponding charge density cut-off of 360 Ry, and the convergence threshold was set to 10 mRy. The converged Monkhost-Pack (Monkhorst and Pack, 1976) (k-point) mesh $8 \times 8 \times 8$ as seen in Figure 2 for the bulk material and $8 \times 8 \times 1$ for the slabs, was used to carry out integration across the Brillouin zone (BZ). The electron occupancies were determined by Marzari Vanderbilt (Panati and Pisante, 2013) as implemented in the QE code. A smearing of 0.005 Ry was identified as optimal for achieving reasonable convergence. The optimization of the total energy for slabs of various thicknesses was performed solely concerning atomic positions, keeping the lattice parameter constant at its equilibrium value of 3.33615 Å, equivalent to diamond FCC Carbon.

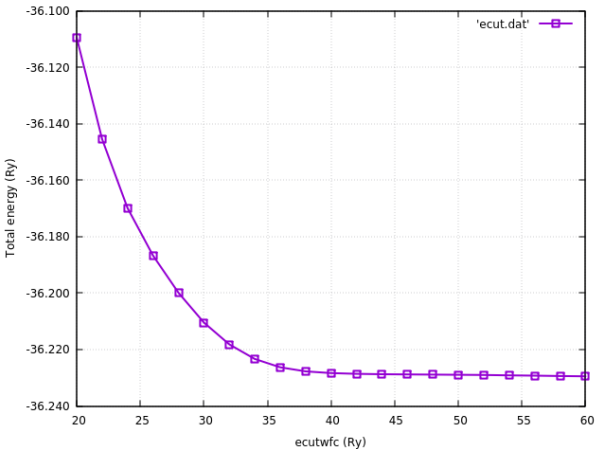

Figure 1: *The wavefunction cut-off energy (ecutwfc) as a function of total energy of bulk diamond.*

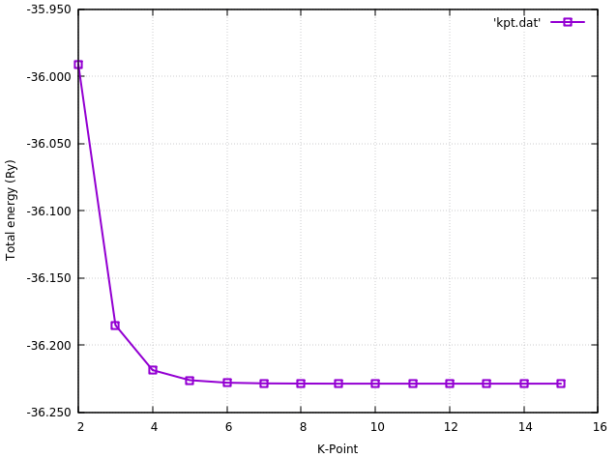

Figure 2: *The K-Point mesh as a function of total energy (Ry) of bulk diamond*

3. RESULT AND DISCUSSION

3.1 Structural Properties of Bulk Diamond Carbon

The diamond cubic structure is formed by the interpenetration of two face-centered cubic lattices, one of which is shifted by a quarter of a cube's length along the diagonal. It can also be depicted as a face-centered cubic lattice in which half of the tetrahedral sites are occupied while the octahedral sites remain unoccupied. The figure 3 displays the unit cell of the diamond cubic structure. In this arrangement, each carbon atom has four neighboring atoms, and the shortest distance between carbon atoms (C-C) can be calculated using the unit cell parameter.

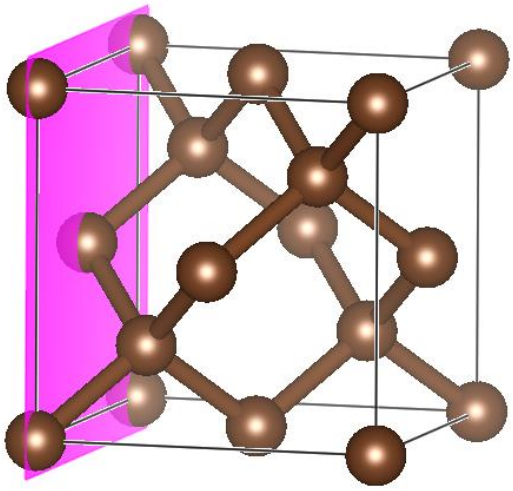

Figure 3: *Unit cell of diamond Carbon with the (100) plane*

Table 1: *Bulk properties of the bulk carbon in diamond structure*

	Lattice Parameter (Å)	**Bulk Modulus (GPa)**	**Pressure Derivative**
Carbon (diamond)	3.556^{a} 3.577^{b}	435.5	75.89

This work [a], Rivero and coworkers[b] (Rivero *et al.*, 2016)

We calculated the lattice parameter and bulk modulus for diamond-like Carbon (see Table 1). The large Bulk Modulus provides information about the toughness of the Carbon material. The computations involve determining the total energy of the bulk across various lattice parameters. The total energy information is then utilized to fit the Murnaghan equation of state (Murnaghan, 1944), deriving the bulk modulus.

$$E = E_0 + \frac{B_0 V}{B_0'}\left[\left(\frac{V_0}{V}\right)^{B'}\frac{1}{B_0'-1}+1\right] - \frac{B_0 V_0}{B_0'-1} \quad (1)$$

where E_0, B_0, B_0', V_0, V are the energy at equilibrium, bulk modulus at equilibrium, pressure derivative of the bulk modulus, equilibrium volume, and given volume of the unit cell crystal.

The bulk modulus describes how the energy changes concerning the volume of a material near its equilibrium state, and it signifies the material's resistance to external pressure. When the bulk modulus is high, as with diamond carbon, the energy versus volume curve is steep. The implication is that even a small change in volume results in a significant change in energy, making it difficult to deform the material.

3.2 Work Function (100) Surface of Diamond Carbon

An understanding of the surface structure and chemical composition is essential for grasping the process of electron emission into vacuum states. The C(100) surface structured with a tetragonal cell with an interlayer distance of 1.778075 Å. The asymmetric slabs consisted of vacuum of 8.8904 Å. Surface relaxation was not considered for the C(100) surface.

The work function of a material generally varies based on the specific orientation of its crystal surface, known as work function anisotropy. It can be described as the energy difference between a neutral crystal and an identical crystal with one electron extracted. This definition assumes a zero temperature and a perfect vacuum, presuming the material is in its ground state before and after the electron removal. The work function is the minimum energy needed to remove an electron from the bulk of a material through the surface to point outside the material, and can be written as:

$$\Phi = V_{\text{vacuum}} - E_{\text{Fermi}} \quad (2)$$

where the potential in the vacuum region V_{vacuum} and the Fermi energy E_{Fermi} are derived from the same calculation.

All the potentials discussed here tail off more rapidly in the vacuum region of the slab-supercell when compared to the full Kohn-Sham potential, including the exchange-correlation potential. We obtained the work function for the different layers from the difference between the potential in the vacuum region and the Fermi energy of the slab.

Figure 4: *Diamond C(100) surface slab*

Using a slab model (Figure 4) reduces the computational time since the entire material or crystal can be computationally expensive. Slab modeling allows scientists to reduce the system's complexity by focusing on a finite portion of the crystal, making simulations more feasible and efficient.

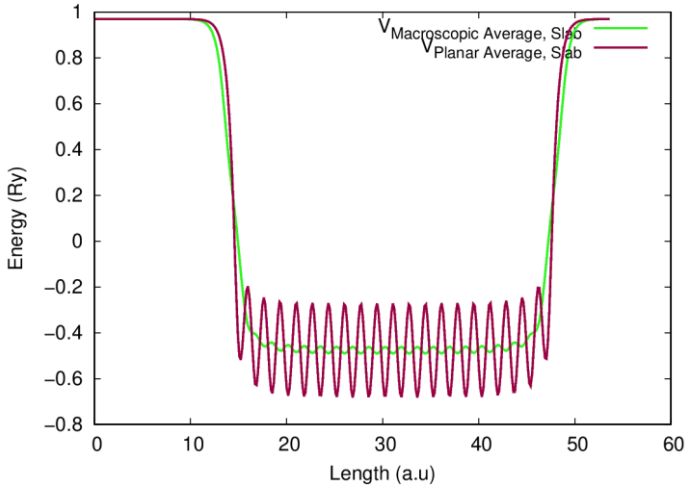

Figure 5: *Potential of the macroscopic average and potential of the planar average for the C(100) with 10 layers of slab thickness of C(100)*

The potential due to the macroscopic average represents the electric potential at a point in space caused by the combined effect of all the charges within a macroscopic volume or region. The macroscopic average for the slab consisting of 10 layers is shown in Figure 5. The electric potential produced by the distribution of charge throughout a two-dimensional planar surface at a specific place in space is known as the potential due to planar average. As shown in Figure 5, it is expected that at a length equal to 0 a.u and a very large length of the slab, the macroscopic and planar averages are expected to coincide.

Table 2: *Work function from different slab thickness of the C(100) surface.*

Thickness of Slab	Vacuum Potential (Ry)	Vacuum Potential (eV)	Fermi Energy (eV)	Work Function (eV)
1	0.154751090	2.1054975206	-4.0356	6.141097
2	0.511838081	6.9639174139	-0.4283	7.392217
3	0.512915099	6.978571002	-0.5834	7.561971
4	0.769699396	10.472302133	2.9432	7.529102
5	0.857694082	11.669531782	4.1295	7.540032
6	0.928082626	12.627217475	5.0803	7.546917
7	0.833822046	11.344735927	3.8008	7.543936
8	0.885461536	12.047327541	4.5079	7.539428
9	0.930248908	12.656691267	5.1196	7.537091
10	0.969336620	13.188507105	5.6527	7.535807
11	1.003575177	13.654346776	6.1193	7.535047
12	1.162980553	15.823169134	8.2890	7.534169
13	1.181849080	16.079888727	8.5896	7.490288
14	1.085128675	14.763939528	7.2310	7.53294
15	1.107355373	15.066349402	7.5332	7.533149

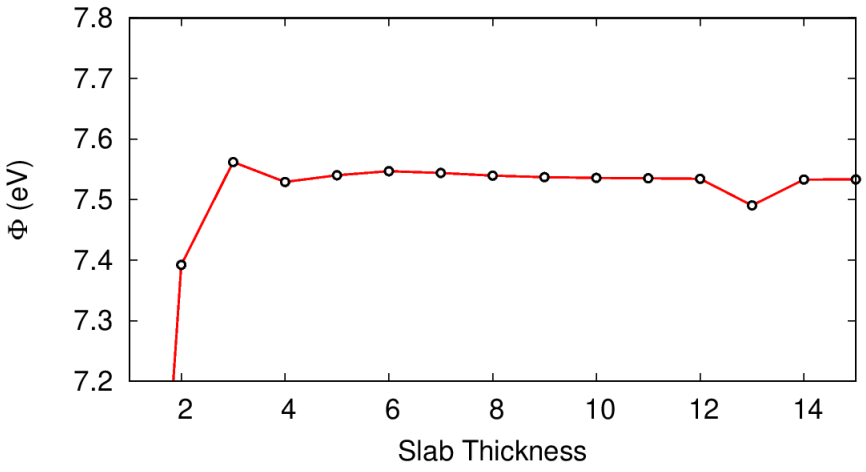

Figure 6: *Workfunction of C(100) versus slab thickness.*

From Figure 6, the obtained work function of C(100) converges at 7.53 eV. The work function of carbon has been experimentally reported as 6.00eV (Diederich *et al.*, 1998) and 5.00 ± 0.60 eV (Kawano, 2022).

The vacuum potential (see column 2 of Table 2) is in a unit of Rydberg (Ry) as obtained from the calculation using the Quantum Espresso codes. The Equivalent of this energy in electron volt (eV) is provided in column 3 of Table 2. The conversation is necessary as the unit of the work function is in eV, as seen in Equation (2).

4. CONCLUSION

Density-functional theory with generalized gradient approximation has been used to study the (100) surface carbon in the diamond structure. The structural properties of the bulk and the work function of C(100) have been calculated and compared with experimental studies. The obtained work function is 7.53 eV, slightly more than the experimental value. The result is at 0K, while the experiment is obtainable at 300K. The effect of temperature, as well as involving surface relaxation and possible surface reconstruction, will improve the result and thus reduce the slight deviation from the experimental value.

ACKNOWLEDGEMENTS

J.O.R. acknowledges CHPC, South Africa, through the MATS1181 project for access to computational resources.

CONFLICT OF INTEREST

No conflict of interest was declared by the authors.

REFERENCES

[1] Diederich, L., Küttel, O. M., Aebi, P., Maillard-Schaller, E., Fasel, R., and Schlapbach, L. (1998). Photoelectron emission from the negative electron affinity caesiated natural diamond (100) surface. *Diamond and Related Materials*, *7*(2–5). https://doi.org/10.1016/s0925-9635(97)00284-7

[2] Endo, K., Koizumi, S., Otsuka, T., Ida, T., Morohashi, T., Onoe, J., Nakao, A., Kurmaev, E. Z., Moewes, A., and Chong, D. P. (2003). Analysis of Electron Spectra of Carbon Allotropes (Diamond, Graphite, Fullerene) by Density Functional Theory Calculations Using the Model Molecules. *Journal of Physical Chemistry A*, *107*(44). https://doi.org/10.1021/jp0345710

[3] Giannozzi, P., Baroni, S., Bonini, N., Calandra, M., Car, R., Cavazzoni, C., Ceresoli, D., Chiarotti, G. L., Cococcioni, M., Dabo, I., Dal Corso, A., De Gironcoli, S., Fabris, S., Fratesi, G., Gebauer, R., Gerstmann, U., Gougoussis, C., Kokalj, A., Lazzeri, M., … Wentzcovitch, R. M. (2009). QUANTUM ESPRESSO: A modular and open-source software project for quantum simulations of materials. *Journal of Physics Condensed Matter*, *21*(39). https://doi.org/10.1088/0953-8984/21/39/395502

[4] Jolayemi, O. R., Adetunji, B. I., Onuorah, I. J., and Idiodi, J. O. A. (2021). First-Principles Study of the Half-Metallic Properties of (001), (110), and (111) Surfaces of RbSe in the CsCl Structure. In *Journal of Electronic Materials* (Vol. 50, Issue 10). https://doi.org/10.1007/s11664-021-09076-3

[5] Kawano, H. (2022). Effective Work Functions of the Elements. *Progress in Surface Science*, *97*(1). https://doi.org/10.1016/j.progsurf.2020.100583

[6] Monkhorst, H. J., and Pack, J. D. (1976). Special points for Brillouin-zone integrations. *Physical Review B*, *13*(12). https://doi.org/10.1103/PhysRevB.13.5188

[7] Murnaghan, F. D. (1944). The Compressibility of Media under Extreme Pressures. *Proceedings of the National Academy of Sciences*, *30*(9). https://doi.org/10.1073/pnas.30.9.244

[8] Olawole, O. C., De, D. K., Olawole, O. F., Lamba, R., Joel, E. S., Oyedepo, S. O., Ajayi, A. A., Adegbite, O. A., Ezema, F. I., Naghdi, S., Olawole, T. D., Obembe, O. O., and Oguniran, K. O. (2022). Progress in the experimental and computational methods of work function evaluation of materials: A review. In *Heliyon* (Vol. 8, Issue 10). https://doi.org/10.1016/j.heliyon.2022.e11030

[9] Olawole, O. C., De, D. K., Oyedepo, S. O., and Ezema, F. I. (2021). Mathematical models for thermionic emission current density of graphene emitter. *Scientific Reports*, *11*(1). https://doi.org/10.1038/s41598-021-01546-2

[10] Panati, G., and Pisante, A. (2013). Bloch Bundles, Marzari-Vanderbilt Functional and Maximally Localized Wannier Functions. *Communications in Mathematical Physics*, *322*(3). https://doi.org/10.1007/s00220-013-1741-y

[11] Perdew, J. P., Burke, K., and Ernzerhof, M. (1996). Generalized gradient approximation made simple. *Physical Review Letters*, *77*(18). https://doi.org/10.1103/PhysRevLett.77.3865

[12] Perdew, J. P., Burke, K., and Ernzerhof, M. (1997). Generalized Gradient Approximation Made Simple [Phys. Rev. Lett. 77, 3865 (1996)]. *Physical Review Letters*, *78*(7). https://doi.org/10.1103/physrevlett.78.1396

[13] Rivero, P., Shelton, W., and Meunier, V. (2016). Surface properties of hydrogenated diamond in the presence of adsorbates: A hybrid functional DFT study. *Carbon*, *110*. https://doi.org/10.1016/j.carbon.2016.09.050

[14] Singh-Miller, N. E., and Marzari, N. (2009). Surface energies, work functions, and surface relaxations of low-index metallic surfaces from first principles. *Physical Review B - Condensed Matter and Materials Physics*, *80*(23). https://doi.org/10.1103/PhysRevB.80.235407